Wall conditioning by ECRH discharges and He-GDC in the limiter phase of Wendelstein 7-X

T. Wauters[1], R. Brakel[2], S. Brezinsek[3], A. Dinklage[2], A. Goriaev[1], H.P. Laqua[2], S. Marsen[2], D. Moseev[2], T. Stange[2], G. Schlisio[2], T. Sunn Pedersen[2], O. Volzke[2], U. Wenzel[2], and the W7-X team

EUROfusion Consortium, JET, Culham Science Centre, Abingdon, OX14 3DB, UK
[1] Laboratory for Plasma Physics, LPP-ERM/KMS, Brussels, Belgium, TEC Partner
[2] Max-Planck-Institute for Plasma Physics, Greifswald, Germany
[3] Forschungszentrum Jülich, Jülich, Germany, TEC Partner

E-mail: t.wauters@fz-juelich.de

Abstract. Wendelstein 7-X (W7-X) relies on wall conditioning to control the density and the impurity content of the plasma. Wall conditioning in the first operation campaign of W7-X consisted of baking at 150°C during 1 week prior to operation, glow discharge conditioning (GDC) in helium and electron cyclotron resonance heating (ECRH) discharges. Additionally, the usage of He-GDC was limited to avoid sputtering and migration of metallic plasma facing components. This presented an unique opportunity for studying the applicability of ECRH discharges for initial wall conditioning on a stellarator, albeit in Carbon limiter configuration. A single envelope curve is observed in the normalised outgassing data that takes into account all ECRH discharges. This illustrates that the majority of the discharges operated at the limits of a radiative collapse. Hydrogen recycling dominated the fuelling of the ECRH discharges throughout while CO outgassing was found strongest at the start of the campaign. A reduction of recycling was observed throughout the campaign. Temporarily depleting the walls from H and impurities was possible by He-GDC. It was shown that the recycling coefficient in H_2-ECRH plasmas could be reduced and the pulse duration significantly extended by He-'recovery' ECRH plasmas. Good wall conditions were defined by normalised outgassing values below 1×10^{-9} mbar/kJ. In absence of H_2-GDC, more than 311 cumulated discharge seconds of ECRH discharges are needed for obtaining lastingly low outgassing levels. A release model with two trapping reservoirs could reproduce the normalised outgassing trend, including ECRH and GDC plasma wall interactions.

1. Introduction

Operation of magnetic confinement fusion devices is largely affected by the surface conditions of the plasma facing components (PFC). The surface properties have a substantial impact on the recycling of particle fluxes that may become much larger and may penetrate deeper into the plasma than particles from other sources (e.g. gas puff). More over, it appears to be self-evident that the release of material from the PFC acts to the plasma as an impurity source that requires ways to suppress or to control. For large stellarators, the requirements on plasma purity and fuelling may even be amplified due to strong neoclassical thermo-diffusion [1]. Therefore, wall conditioning is a prerequisite to attain good plasma performance.

Wall conditioning is commonly applied in magnetic controlled fusion devices to control the surface state of the PFC [2]. It is relied upon in the Wendelstein 7-X (W7-X) operation phases to control the density and the impurity content of the plasma, with the eventual aim of providing access to steady state operation scenarios at 10 MW [3]. The super-conducting stellarator W7-X keeps its magnetic field charged throughout an experimental day. Conventional wall conditioning by glow discharges therefore cannot be used routinely between plasma experiments. Alternatively Radio Frequency (RF) -based wall conditioning scenarios compatible with the magnetic field are foreseen. The multi-megawatt Electron Cyclotron Resonance Heating (ECRH) system [10], operational during the first operation campaign (OP1.1) of W7-X, is well suited for RF conditioning. The confining vacuum magnetic field configuration of the stellarator already exists in the vacuum. The ECRH conditioning plasma can therefore be easily made sufficiently dense and hot to provide good absorption of ECRH power. Conditioning by RF discharges in the Ion Cyclotron Range of Frequency (ICRF) is planned for future operation campaigns.

This contribution analyses the performance improvement of W7-X plasmas by means of Electron Cyclotron Wall Conditioning (ECWC) and Glow Discharge Conditioning (GDC) throughout OP1.1. It reports on the very first systematic application of ECWC on a large stellarator. A pre-study was performed on the smaller Hybrid-experiment WEGA (both tokamak and stellarator operation is possible) [4]. ECWC was studied extensively for the tokamak vacuum magnetic field configuration on TCV [5], TOMAS [6], TORE SUPRA [7], KSTAR [8] and JT60-U [9]. However, unlike on tokamaks, ECWC on stellarators does not suffer from poloidal inhomogeneity or potentially high levels of non-absorbed ECRH radiation. Common challenges for tokamaks and stellarators are increasing the plasma wetted area of the ECRH discharge [4].

OP1.1 made no clear distinction between ECWC and other (ECRH) discharges, neither in terms of discharge gas, fuelling scheme, magnetic field configuration, heating scheme nor heating power. Therefore we omit in this paper the specific term ECWC and speak more generally about conditioning by ECRH discharges. Indeed, each performed ECRH discharge has contributed to the observed gradual changes in wall conditions

throughout OP1.1, described in this paper. The ECRH system operated at $f = 140\,\mathrm{GHz}$ with second-harmonic absorption at $B_0 = 2.5\,\mathrm{T}$. Nearly all ECRH discharges of OP1.1 are performed in limiter magnetic field configuration on 5 inertially cooled graphite limiters (figure 1(a-b)) [11] representing a total surface area of $0.86\,\mathrm{m}^2$. Other installed PFC's are composed of stainless steel protection panels ($70\,\mathrm{m}^2$) and CuCrZr heat sink structures ($\sim 45\,\mathrm{m}^2$) [12], of which maximum 20% are covered by carbon protection tiles (figure 1(b)). The vessel is kept at room temperature. The free volume is about $110\,\mathrm{m}^3$ with a plasma volume of $30\,\mathrm{m}^3$. Vacuum is provided by 30 turbo molecular pumps with an effective pumping speed in the vessel of about $40\,\mathrm{m}^3/\mathrm{s}$ for H_2 [13]. GDC is operated between experimental days when the magnetic field coils are de-energised. Overall, the usage of GDC was limited to avoid sputtering on the unprotected CuCrZr structures. A total of 10.9 h of GDC is performed throughout the campaign, in He only. The experimental arrangement for GDC on W7-X involves 10 graphite DC anodes, one per half module, operated at max. 1.5 A per anode [14]. 9 out of 10 anodes were operational.

Vacuum vessel and PFC conditioning of W7-X prior to plasma operation consisted of 1 week of baking at 150°C without any GDC. As such, many plasma impurities such as oxygen, carbon-oxide, water etc. were expected. This presented a unique opportunity for studying the applicability of ECRH discharges for initial wall conditioning on a stellarator. It is to be noted that similar initial conditions would have prevented sustained breakdown of ohmic plasma on a tokamak, even with ECRH start-up assistance. Start-up in a tokamak is incompatible with poorly conditioned PFC's. Tokamak plasma in the breakdown, burn through and current ramp-up phase is poorly confined. Impurity release from the surfaces by the inevitable convective fluxes to the PFC's would lead to unsustainable radiation power losses. ECRH discharges are produced by absorption of RF power at the electron cyclotron resonance condition that

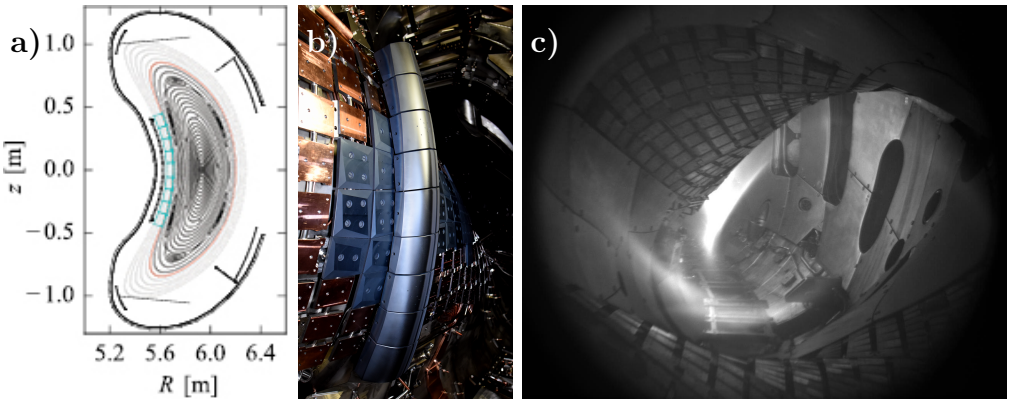

Figure 1: (a) Poincaré plot taken from [15] showing the flux surfaces of the OP1.1 limiter configuration. The limiter is marked in blue while the last closed magnetic surface (LCFS) is indicated in red. (c) W7-X PFC in OP1.1: Photo taken from [16] showing one of five inboard graphite limiters and CuCrZr heat sink structures which are partially covered by graphite tiles. (c) CCD image of W7-X He-ECRH discharge 20160310.025 (see also figure 6) at 2 MW, tangential view from port AEQ51.

on a stellarator locates inside of the confining nested magnetic flux surfaces. Fully ionised plasma can be obtained inside of the confined region before the first convective fluxes reach the PFC's. Hence, the performance of W7-X with limited initial conditioning was remarkably good from the start of OP1.1 on. This is by no means a reason to spare on initial conditioning. The here presented analysis stresses the importance of wall conditioning and contributes to the development of the conditioning strategies for future operation campaigns on W7-X. The presented results of ECRH discharges and He-GDC in limiter configuration on W7-X are as well directly transferable to tokamaks. Indeed, the majority of the convective fluxes in ECRH conditioning plasma on a tokamak will be received by the first field line intersecting components such as poloidal protection limiters.

2. Normalised outgassing

Within the context of this paper, the W7-X plasma performance is evaluated by following parameters: (i) plasma discharge duration, (ii) injected energy and (iii) outgassing pressure peak at the end of the discharge. The latter is considered to be proportional to the release rate of gas from the PFC's at discharge ending. Figure 2 shows the evolution of the outgassing pressure peak normalised to the injected energy as a function of the cumulated discharge duration of W7-X ERCH plasmas in the initial He-phase of the campaign. At the start of the campaign, the normalised outgassing was of order 5×10^{-6} mbar/kJ. This number denotes that on average 10 kJ of ECRH energy could be injected in a 10 ms plasma, before the discharge terminates by a radiative collapse producing an outgassing peak of $\sim 5 \times 10^{-5}$ mbar. Mass spectrometry showed a strong release of CO as well as H_2. Outgassing of H_2O and hydrocarbons ($m/z = 16$ or CH_4 in figure 3, with m the mass number and z the charge number) occurred at lower rates. CO remained the dominating impurity throughout the campaign both in H_2 ECRH plasmas as in He discharges ($m/z = 28$ on figure 3). No ion saturation current was observed on the limiter Langmuir probes while the limiter temperature in the first W7-X discharges rose less than 2 °C. The gas release is therefore thought to be triggered on all PFC's by photon stimulated desorption and impact of reactive low energy Franck-Condon atoms (~ 2.2 eV) stemming from electron impact dissociation of wall-released molecules such as H_2 or CO. Within 30 to 45 s of cumulated discharge time, the normalised outgassing improves to 3×10^{-8} mbar/kJ, allowing sustaining 0.1 s pulses while injecting ~ 2.5 MW, producing an outgassing peak of $\sim 1 \times 10^{-5}$ mbar.

It is clearly seen on figure 2 that short He-GDC leads to He-ion-induced desorption of hydrogen and intrinsic impurities. This results in de-saturated wall components evidenced by a temporary improvement of the outgassing and, as a consequence, of the discharge performance. Similar observations have been made on tokamaks TEXTOR [17] and DIII-D [18] with carbon PFCs. Wall conditioning by He-GDC provided access to 0.5 s pulses and 2 MJ of injected power per pulse towards the end of the He-phase, successfully concluding the first half of the very first operation campaign of W7-X.

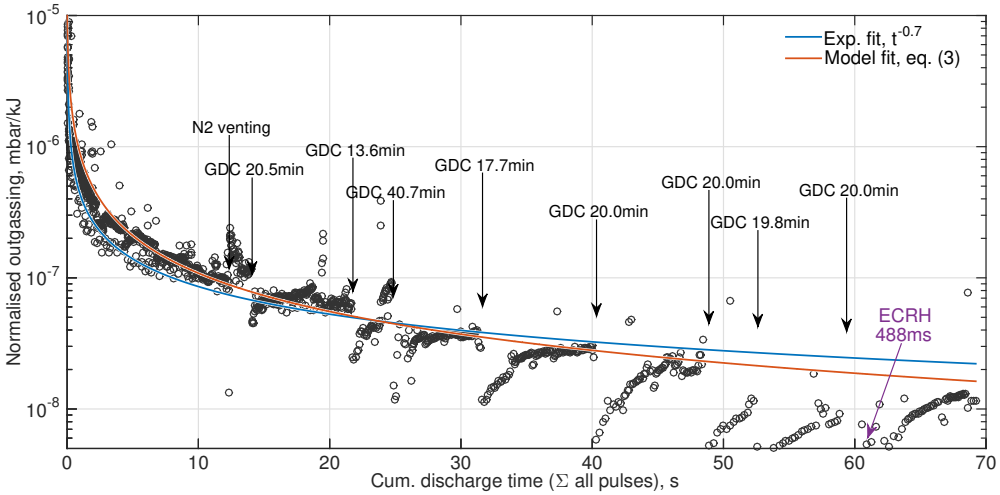

Figure 2: Normalised outgassing in subsequent He ECRH discharges (20151211.1 to 20160128.27) as function of the cumulated ECRH discharge duration: experimental data (circles) overlaid with typical experimental $t^{-0.7}$ trend (blue line) and fitted by eq. 3 (red line, see section 3). The discontinuities in the data trend result from He-GDC operation, indicated by arrows.

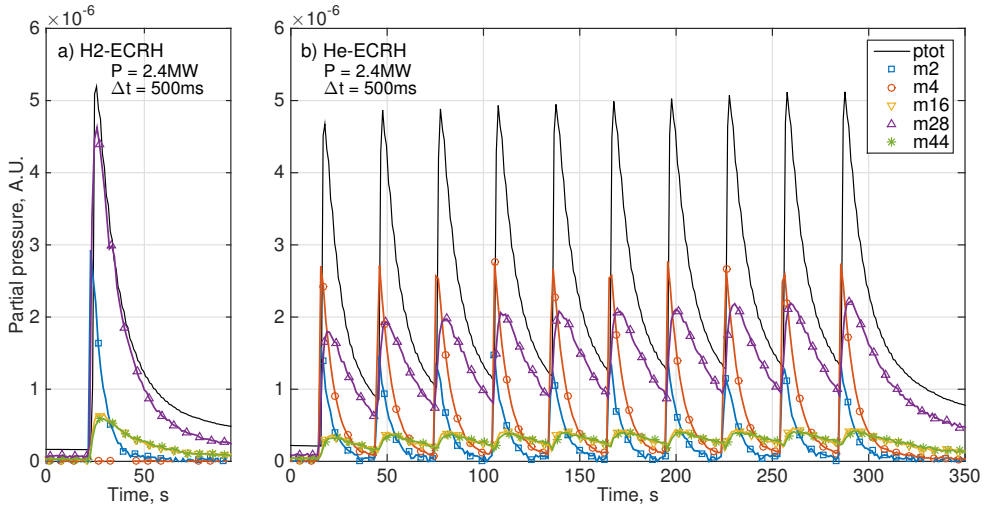

Figure 3: Typical mass spectrometry time traces, for a) H_2 ECRH (20160209.004) and b) He-ECRH (20160209.005) discharges in OP1.1. The H_2 ($m/q = 2$) and He ($m/q = 4$) traces are calibrated by dry gas puffs, while traces $m/q = 16$ (CH_4), $m/q = 28$ (CO, N_2) and $m/q = 44$ (CO_2) are scaled, all with the same factor, to reproduce tentatively the total pressure (black solid line). The total pressure (black) is an average over a set of ionisation gauges in the pumping ducts. The mass spectrometer is localised in one of these pumping ducts and features therefore similar conductivity to the main vessel as the pressure measurements.

3. Model for conditioning by ECRH discharges and He-GDC

The normalised outgassing trend corresponds to the typical $t^{-0.7}$ dependence (blue line, figure 2), observed also on JET (Carbon & ITER-Like Wall [19]), TORE SUPRA [20]

and other devices [21]. The power law originates from processes such as included in Andrew's model [22], that derives from trapping site concentrations, detrapping, retrapping and recombination to molecule. We repeat below the main equations of the model, eq. 1 and eq. 2 [22]:

$$\frac{\partial c_t}{\partial t} = -K_{ts}c_t + K_{st}c_s\left(1 - \frac{c_t}{c_0}\right) \tag{1}$$

$$\frac{\partial (c_t + c_s)}{\partial t} = K_r c_s^2 \tag{2}$$

They essentially represent the exchange of atoms (e.g. H) between two states t and s, where the first typically represents deeply trapped atoms and the second loosely bound atoms (solution). K_{ts} and K_{st} are the rate constants associated with detrapping from t into s and retrapping respectively. The possible concentration c in state t is finite and limited by c_0. The release rate of gas is $K_r c_s^2$ and occurs from state s with (recombination) rate K_r. When $c = c_t + c_s \approx c_t$, then the outgassing rate is approximated by eq. 3 with $K = K_r(K_{ts}/K_{st})^2$. [22]

$$\frac{\partial c}{\partial t} \approx -K\frac{c^2}{\left(1 - \frac{c}{c_0}\right)^2} \tag{3}$$

The outgassing rate following from eq. 3 is plotted in red on figure 4 with $Kc_0 = 10^{-2}\,\mathrm{s}^{-1}$ and $c(t = 0) = 0.95c_0$. The data points represent the experimental normalised

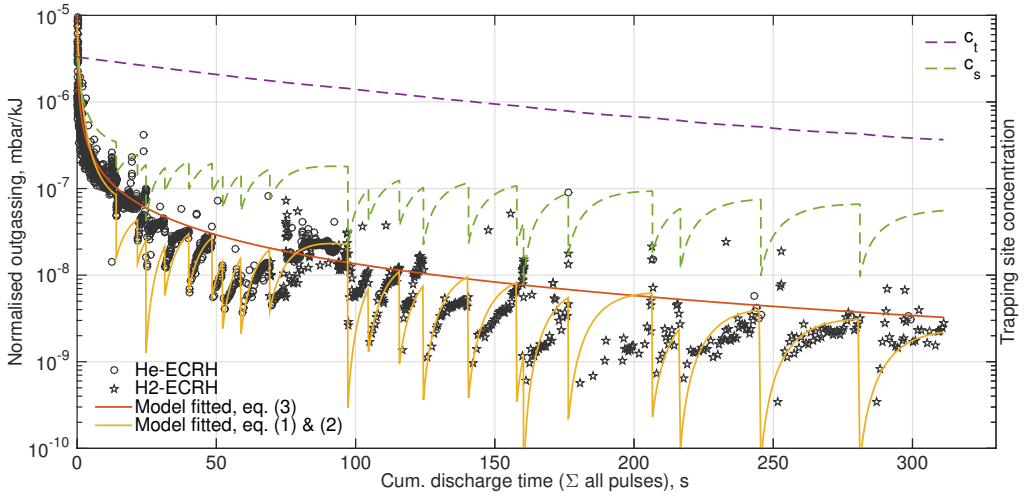

Figure 4: Left axis: Normalised outgassing throughout OP1.1: experimental data of He and H_2-ECRH discharges (circles and pentagrams resp.), fit using eq. 3 (red line) and fit using eq. 1 and 2 including the conditioning contribution by GDC (yellow line). Right axis: Trapping site concentrations in particle reservoirs t (purple) and s (green) following from latter (yellow) fit.

outgassing data for every ECRH pulse in the OP1.1 campaign. He discharges and H_2 discharges are indicated by circles and pentagrams respectively. It is clear that the He discharges, mainly in first part of the campaign, and the H_2 discharges, mainly

in the second part of the campaign, follow the same trend (red line). As such it is concluded that outgassing from the PFC's has continued to play a major role in the fuelling of the plasma throughout the second phase. The trend line of the normalised outgassing decreased to an average value of 3×10^{-9} mbar/kJ towards the end of the campaign. Values below 10^{-9} mbar/kJ have been obtained in this phase after He-GDC and allowed to sustain 6 sec plasma pulses at low ECRH power, staying within the (in OP1.1) maximum allowed 4 MJ [11] of energy. The limiter surface temperatures reached values of several hundreds of °C in these discharges [3] with a steady bulk temperature throughout the day of 70 to 120 °C [16]. It is therefore considered that at this stage the limiter surfaces have been properly conditioned by the convective heat flux from the plasma on the surface. The gradual deterioration of the normalised outgassing towards the main trend line after a He-GDC can then be attributed to particle release from the other PFC's.

Further exploring the outgassing rate by eq. 1 and 2 illustrates the distinct effects of He-GDC and ECRH discharges on the trapping site concentrations. The result is plotted in yellow on figure 4. The curve includes the discontinuities that are produced by short (5 to 40 mins) He-GDC. The experimentally observed normalised outgassing rate could be reproduced by making following assumptions: The decrease in time of $c_t + c_s$ defines the release rate of molecules from the walls. The volume of the W7-X vacuum vessel relates the number of molecules to pressure. Considering an averaged ECRH power of 3 MW in OP1.1 retrieves the normalised outgassing rate. The rate constants during H_2 and He ECRH plasmas are fixed at $K_r = 3 \times 10^{-24}$, $K_{ts} = 0.01$ and $K_{st} = 0.05$ (resulting in $Kc_0 = 4 \times 10^{-2}\,\mathrm{s}^{-1}$). The initial concentration for sites t and s are set $c_t(t = 0) = c_s(t = 0) = 3.3 \times 10^{23}$. He-GDC removes atoms from state s only, setting $K_{ts} = K_{st} = 0$ during the GDC. The removed amount of atoms by a GDC procedure is estimated as $\int I_{GDC} Y_{GDC} c_s \mathrm{d}t$, with the glow current I_{GDC} measured at the DC generators and Y_{GDC} the physical sputtering yield by He ions, that is used here as a constant fitting parameter ($Y_{GDC} = 3 \times 10^{-5}\,\mathrm{C}^{-1}$ in range of [23], i.e. $< 2 \times 10^{-4}\,\mathrm{C}^{-1}$). The total removal from the trapping sites after 311 s of cumulated discharge time is estimated from this analysis at $c_t + c_s \approx 6.2 \times 10^{23}$ atoms, or 3.1×10^{23} (H_2) molecules.

The time evolution of the trapping site concentrations modelled by eq. 1 and 2 are shown on the right axis of figure 4 in purple (c_t) and green (c_s) respectively. It is concluded from these curves that hydrogen/impurity removal from c_t by ECRH discharges is a slow (factor 10 in 311 s) but necessary process. Depleting c_s by He-GDC has little effect on c_t in the subsequent ECRH discharges, but it results in a temporary improvement of the normalised outgassing and therefore also of the achievable injected energy levels. Long pulse operation on W7-X may require a strongly depleted c_t as nearly all ECRH discharges ended with a radiative collapse due to too strong outgassing by the PFC's. It is to be noted that the c_t reservoir may be effectively accessed by H_2-GDC or ICRH conditioning respectively without and with charged magnetic field coils, which hence present itself as a strong recommendation for future campaigns.

4. Gas balance

The total amount of removed atoms by He-GDC and ECRH discharges was estimated in the previous section through a trapping site concentration model. Here the numbers are benchmarked against the balance of injected and pumped amount of gas. Figure 5 presents the gas balance per experiment. An experiment consist of one or a sequence of launched ECRH pulses, as respectively illustrated on figure 2 a) and b). The injected amount of gas (blue) is obtained by integrating the calibrated gas flows corrected for the gas type (He, H_2 or Ar). The pumped amount of gas (red) in each experiment is obtained by the integral of the neutral pressure time traces including discharge and post-discharge phase, multiplied by the pumping speed. Accounting for the gas composition of the residual gas was not feasible. In figure 5 it is assumed that the majority of the outgassed species consist of H_2 molecules. An upper value for CO removal can be estimated by correcting the pumped gas amount for the ionisation gauge sensitivity factor ($S^i_{H_2}/S^i_{CO} \approx 2$ [24]) and the effective pumping speed of CO at W7-X (e.g. $S^p_{H_2}/S^p_{CO} \approx 4$ for the case where the difference in pumping rate is mainly due to vacuum conductance).

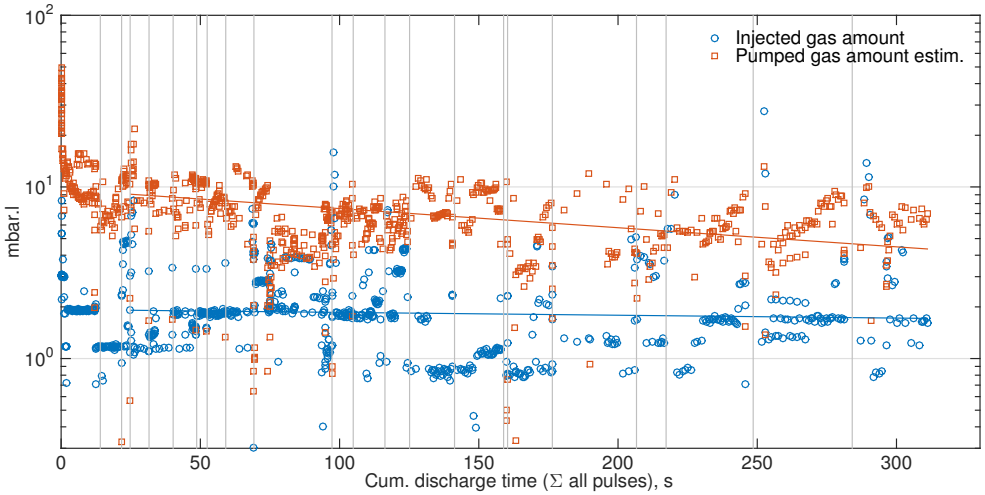

Figure 5: Gas balance per experiment throughout OP1.1 (may include multiple ECRH pulses) as a function of the cumulated RF discharge time for all OP1.1 ECRH plasma experiments. Blue: injected amount (He, H_2 and Ar), red: pumped amount assuming H_2. Both the injected and pumped amounts are normalised to the number of ECRH pulses per experiment.

The balance shows that throughout the campaign on average ~ 5 times more gas is pumped than injected when assuming light species such as H_2: the total injected gas is about 4.4 bar.l, while the pumped amount is about 22 ± 2.2 bar.l. The error estimation accounts for the remaining variation of the effective H_2 pumping speed observed from pulse to pulse in gas injections without plasma, after correcting for the number of connected turbo pumps and their rotation speeds. The net removed amount corresponds to 4.3×10^{23} molecules, in close agreement with the number obtained in the above

analysis. Recycling is closer to 1 after He-GDC, indicated on the time axis by thin vertical grey lines. A slight improvement of recycling can be observed throughout the campaign, indicated by the logarithmic fits in red and blue for the pumped amount of gas and the injected amount of gas respectively.

5. Helium ECRH recovery discharges

With the W7-X superconducting magnets being powered throughout the experimental day, the best plasma performance was obtained in the first ECRH discharges following the He-GDC operation. Hereafter conditions gradually deteriorated explained by the replenishment of reservoir c_s by atoms from c_t. Towards the end of the first operations campaign however, with normalised outgassing in the range of 3×10^{-9} mbar/kJ (figure 4) or lower and improving recycling (figure 5), it was shown that recycling conditions could be recovered between GDC's by He-ECRH recovery pulses. Figure 6 (a) shows

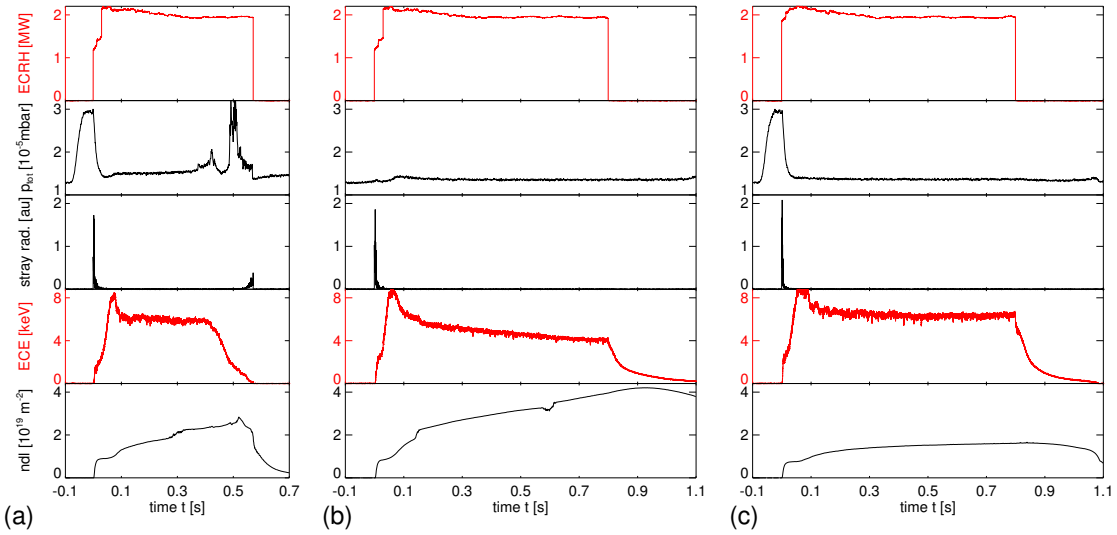

Figure 6: Recovery of recycling conditions in H_2-ECRH plasma by He-ECRH pulses. (a) H_2-ECRH ending by a radiative collapse at 0.575 s (20160310.024). (b) One of two subsequent He-ECRH recovery pulses (20160310.025-026). (c) Recovered H_2-ECRH plasma operation with stable density and temperature throughout the 0.8 s pulse (20160310.027).

a H_2-ECRH plasma with steadily increasing density, ending by a radiative collapse at 0.58 s. The discharge ending is preceded by a pressure increase, as observed by the in-vessel manometer (2^{nd} subplot). Hereafter the plasma cools down (4^{th} subplot) leading to a loss of ECRH power absorption. An increased level of ECRH stray radiation (3^{rd} subplot) due to non-absorbed power triggers then a safety interlock that stops the ECRH gyrotrons (1^{st} subplot).

The plots of figure 6 (b) show the first of two He-ECRH recovery pulses. The helium discharge removes hydrogen and impurities from the plasma facing components without retaining significant amounts of helium. Figure 6 (c) shows the subsequent H_2-ECRH plasma operation with stable density and temperature throughout the 0.8 s

pulse. It shows that the recycling coefficient could be reduced and the pulse duration significantly extended by He-ECRH conditioning.

6. Outlook to divertor operation on W7-X

The divertor configuration has a clear advantage over the limiter configuration for impurity shielding as well as for hydrogen recycling. Particles recycling from a limiter surface easily enter into the LCFS as neutrals while this is far less probable in case of a divertor. The divertor surfaces that receive the main particle flux, the targets, are located away from the confined plasma [26]. It can therefore be expected that the divertor configuration is more resilient to particle release from the PFC's. The first ECRH pulse with good RF power absorption in the first divertor campaign on W7-X was preceded by 1 week of baking at 150°C as in OP1.1, 160 minutes of H_2-GDC and 35 minutes of He-GDC. The impurity mass spectrometry traces dropped by more than one order of magnitude during the H_2-glow. Hence, impurity release from the PFC's in the first divertor pulse was expected to be less severe than in the first limiter pulses. Indeed, the normalised outgassing of the first divertor ECRH pulse (H_2) was 3.5×10^{-8} mbar/kJ, significantly better than in the first limiter plasmas. A steep increase of the normalised outgassing throughout an experimental day could be observed in the first divertor operation days. However, outgassing was significantly lowered from day to day by further H_2-GDC conditioning followed by He-GDC between these experimental days. The normalised outgassing could be reduced to values around 1×10^{-9} mbar/kJ within three days, where after it hovered around this value for the remainder of the campaign.

The significant difference in performance compared to OP1.1 results in part from the divertor configuration being more resilient to particle recycling. It has to be considered however that without the application of H_2-GDC for initial conditioning in this divertor campaign, a comparable amount of impurities as at the start of OP1.1 would have resided on the PCF?s, with inevitable unfavourable impact on performance. These results therefore confirm the thesis of this paper that ECRH conditioning combined with He-GDC is not well suitable for the initial discharge conditioning of W7-X.

7. Conclusion

Wall conditioning in the limiter campaign of W7-X consisted of (i) baking at 150°C during 1 week prior to operation, (ii) He-GDC conducted in between operation days and (iii) ECRH discharges. The usage of He-GDC was limited to avoid sputtering and migration of metallic PFC's. This allowed us to study the applicability of ECRH discharges for initial wall conditioning on a stellarator. The OP1.1 limiter ECRH pulses were characterised by low plasma purity and density control. Hydrogen recycling dominated the fuelling of the ECRH discharges throughout OP1.1 while CO outgassing was found strongest at the start of the campaign. A release model with two trapping

reservoirs could reproduce the outgassing trend of the entire campaign, including the distinct effects of ECRH and He-GDC plasma wall interactions. More than 311 cumulated discharge seconds of ECRH discharges were needed to sufficiently deplete reservoir c_t and obtaining lastingly low outgassing levels. Temporarily depleting the walls from H and impurities was possible by He-GDC, and results from the depletion of reservoir c_s. Good wall conditions that sustain 4 MJ discharges, were defined by normalised outgassing values below 1×10^{-9} mbar/kJ. These conditions have been obtained in the first ECRH discharges after He-GDC operation, where after conditions gradually deteriorate explained by the replenishment of reservoir c_s by atoms from reservoir c_t. The majority of pulses in OP1.1, in limiter configuration and with limited pre-conditioning, had however higher normalised outgassing. The majority of the discharges operated at the limits of radiative collapses. This defined the observed single envelope curve for the normalised outgassing data points throughout the campaign. In next operation phases, with the limiters replaced by divertors and the CuCrZn cooling structures fully protected by carbon tiles, long GDC in H_2 will be operated to deplete the walls from impurities (CO, CO_2 and H_2O).

It is concluded that ECRH discharges in helium or hydrogen combined with He-GDC, are not ideally suited for the purpose of initial conditioning of W7-X. Obtaining lastingly low outgassing levels by ECRH conditioning in limiter configuration proved to be time consuming as the pulse duration of an (X2-)ERCH discharge is limited by outgassing. The released impurities cool the plasma below the cut-off for ECRH power absorption. ICRH conditioning overcomes this difficulty. ICRF waves couple efficiently to low density, low temperature plasma, even in the presence of impurities, and at full operating magnetic field in W7-X. For this reason it may as well operate at an order of magnitude higher gas throughput. ICWC might therefore be a preferred method for wall conditioning in future operation phases of W7-X. The scope of ECRH conditioning for future campaigns was illustrated toward the end of OP1.1. With the improved wall conditions it was shown that the recycling coefficient in H_2-ECRH plasmas could be reduced and the pulse duration significantly extended by He-'recovery' ECRH plasmas.

Acknowledgments

This work has been carried out within the framework of the EUROfusion Consortium and has received funding from the Euratom research and training programme 2014-2018 under grant agreement No 633053. The views and opinions expressed herein do not necessarily reflect those of the European Commission.

References

[1] H. Maaßberg et al., Plasma Phys. Control. Fusion 41 (1999) 1135.
[2] J. Winter, Plasma Phys. Control. Fusion 38 (1996) 1503.
[3] R. Wolf and Wendelstein Team, Fusion Eng. Des. 83, 990 (2008).
[4] T. Wauters et al., AIP Conf. Proc. 1580 187 (2014)

[5] D. Douai et al 2018 Nucl. Fusion 58 026018
[6] A. Goriaev et al., Proc. of the 44th EPS Conference on Plasma Physics P1.117 (2017)
[7] E. Gauthier et al., Proc. of the 28th EPS Conference P5.094 (2001)
[8] K. Itami et al., Journal of Nuclear Materials 438 (2013) S930-S935.
[9] K. Itami et al., Journal of Nuclear Materials 390?391 (2009) 983?987
[10] V. Erckmann et al., Fusion Science Techn. 52, 291 (2007).
[11] T. Sunn Pedersen et al., Physics of Plasmas 24, 055503 (2017).
[12] J. Boscary et al. Fusion Engineering and Design 86 (2011) 572-575
[13] H. Grote et al, Journal of Nuclear Materials 313?316 (2003) 1298-1303
[14] A. Spring, Fusion Eng. and Des. 66-68, 371-375 (2003).
[15] T. Sunn Pedersen et al 2015 Nucl. Fusion 55 126001
[16] G.A. Wurden et al 2017 Nucl. Fusion 57 056036
[17] J. Winter et al., Journal of Nuclear Materials 93 & 94 (1980) 812-819.
[18] G. L. Jackson, Nuclear Fusion, Vol. 30, No. 11 (1990).
[19] V. Philipps et al., Journal of Nuclear Materials 438 (2013) S1067?S1071.
[20] S. Panayotis et al., Journal of Nuclear Materials 438 (2013) S1059?S1062.
[21] M. Mayer et al., Journal of Nuclear Materials 290-293 (2001) 381-388.
[22] P. Andrew and M. Pick, Journal of Nuclear Materials 220-222 (1995) 601-605.
[23] H. F. Dylla, AIP Conf. Proc. 199 3 (1990)
[24] K. Jousten, CERN open-2000-271 20/Aug/2000 (2000)
[25] T. Wauters, ECA Vol. 40A P4.047 (2016)
[26] R. Janev, Atomic And Molecular Processes In Fusion Edge Plasmas, Springer US, 10.1007/978-1-4757-9319-2 (1995)